# Electrochemical Behavior of Nanostructured Nickel Phthalocyanine (NiPc/C) for Oxygen Reduction Reaction in Alkaline Media

Lei Ding[1], Jinli Qiao[1*], Hui Li[2], Haijiang Wang[2*]

[1]College of Environmental Science and Engineering, Donghua University,
2999 Ren'min North Road, Shanghai 201620, P. R. China
[2]Institute for Fuel Cell Innovation National Research Council Canada, 4250
Wesbrook Mall Vancouver, BC, Canada V6T1W5

ABSTRACT

Carbon-supported nickel phthalocyanine (NiPc/C) nanoparticle catalysts have been synthesized by a simple solvent-impregnation and milling procedure, then heat-treated at 600, 700, 800 and 900°C to optimize their activity for the oxygen reduction reaction (ORR). The electrocatalytic activity and electron transfer mechanism of NiPc/C catalysts were demonstrated in oxygen-saturated alkaline electrolyte by cyclic voltammetry (CV), linear sweep voltammetry (LSV) as well as rotating disk electrode (RDE) technologies, respectively. The results show that the heat-treatment temperature has a remarkable impact on the ORR activity of NiPc/C. In particularly, an onset potential of 0.05 V and a half-wave potential of -0.15 V are achieved in 0.1 M KOH after the catalyst was heat-treated at 800°C. In addition to an increase in ORR kinetics the number of electrons transferred for ORR also increased from 2.2 to 2.8 with increasing heat-treatment temperature from 600 to 800°C. To understand the heat-treatment effect, X-ray diffraction (XRD), transmission electron microscopy (TEM), thermogravimetric analysis (TGA) and X-ray photoelectron spectroscopy (XPS) were used to identify the catalyst structure and composition. XPS analysis clearly shows that after the sample was heat treated at 800°C, pyridinic-N and graphitic-N were observed. Both of these species might be assigned to sites catalytically active towards the ORR leading to activity enhancement.

## 1. Introduction

Proton-exchange membrane (PEM) fuel cells as efficient energy conversion devices, have been considered one of the most promising clean powder sources [1,2]. However, despite over a century of study and decades of intensive research, the cost of PEMFCs still inhibits its large scale commercialization. Recently, alkaline fuel cells (AFC) have appeared to be the most promising power source on a cost basis [3-5]. This kind of fuel cell uses an alkaline electrolyte, where the oxygen reduction reaction (ORR) is much faster than in the acidic media of an acidic PEM fuel cells. The faster ORR kinetics in alkaline media makes it possible to use non-Pt catalysts to achieve desirable kinetics for ORR and the high stability of the electrode material afforded. In addition, the use of non-Pt catalysts can effectively reduce the cost of the fuel cell system [6,7].

Due to the advantages associated with alkaline fuel cell systems, significant interests have been evoked on the development of non-Pt catalysts including various transition metals and macrocyclic complexes [8,9]. Among these catalysts, heat-treated metal-N4 macrocycles (MN4), such as phthalocyanine (MPc) complexes and porphyrins, have been considered the most promising ORR catalysts because of their conjugated structure and good chemical stability [10-13].

For pyrolyzed transition metal macrocycle catalysts, it has been reported that four ingredients are required to make well-performing ORR catalysts that exhibit both ORR catalytic activity and stability: transition metal, nitrogen coordinators on these catalysts, carbon support and the process of pyrolysis [14]. With respect to transition metal, macrocycles with different transition metals may display diverse activities, and the electrocatalytic activity of various transition metals follows the order of: $Fe^{2+} > Co^{2+} > Mn^{2+} > Ni^{2+}$, $Cu^{2+}$ [15]. Co- and Fe-centered phthalocyanines are thus popular non-noble metal catalysts that have attracted significant efforts due to their reasonable activity and remarkable selectivity towards ORR in both acidic and alkaline electrolytes [16-20]. Nevertheless, little attention has been given to other metal centered phthalocyanines in the past decades because of the fact that, in strong acidic conditions, such as in PEM fuel cell operating conditions, both activity and stability are much more difficult to achieve. For example, Jun-ichi *et al* [21] reported a procedure to prepare the ORR catalysts using Li- and Mg-phthalocyanines as nitrogen doping agents, but their ORR activities are still lower than those of Co- and Fe-centered phthalocyanines. Most recently, Tebello *et al* [22] measured the ORR activity of several types of Mn-phthalocyanine complexes tetra-substituted with different peripheral ligands. By changing the pH value of solution from 1-12, they found that the electron transfer number per oxygen molecule in the overall reduction process was $2e^-$ in acidic or slightly alkaline media, but $4e^-$ in alkaline media.

In view of these facts, we speculated that other metal centered phthalocyanines could show high catalytic activity towards ORR when changing the electrolyte from acidic to alkaline. In this work, carbon-supported nickel pthalocyanines (NiPc/C) as a typical target was studied as cathode catalyst after heat-treatment. Both electrochemical measurements and physical characterization were performed to study its electrocatalytic activity and its structure and morphology. In case of electrochemical measurements, CV and LSV techniques were employed to investigate the

electrocatalytic activity of NiPc/C heat-treated at different temperatures. RDE theory was used to clarify the ORR mechanisms of NiPc/C with increasing the heat-treatment temperature. With respect to physical characterization, TEM and XRD and TG were conducted to determine the structure and morphology of NiPc/C at different temperatures. In addition, XPS was used to detect surface structure changes and shed some light on the nature of the active centers of the catalyst.

## 2. Experimental

### *2.1 Materials and catalyst preparation*

Nickel phthalocyanine (NiPc) was purchased from Sigma-Aldrich with 97% purity and used as received without further purifications. Carbon Black (Vulcan XC-72, 254 $m^2\ g^{-1}$) was purchased from Cobat Corporation and used as support for all catalysts. In order to disperse the catalysts on the surface of carbon black, 0.4 g NiPc and 0.6 g Vulcan XC-72 were mixed with 100 ml ethanol under constant milling in a mortar for about 2 hrs to obtain a uniform mixture. This mixture was then dried in vacuum at 40°C for about 1 hr to remove ethanol. After drying, the resulting powder was divided into four parts and heat-treated at 600, 700, 800 and 900°C for 120 min under $N_2$ atmosphere, respectively. For convenience, the catalysts heat-treated at different temperatures were denoted as NiPc/C-600, -700, -800, and -900, respectively. $H_2$Pc/C as a reference was also synthesized using the same procedure.

### *2.2 Physical characterization*

TG analyses were carried out on a NETZSCH simultaneous thermal analyzer TG 209. Catalysts samples of about 10 mg were loaded into an alumina pan, and then heated from 25 to 900°C at a rate of $10^oC\ min^{-1}$. All measurements were conducted under nitrogen. The vacant alumina pan was used as a referece throughout the whole experiment.

The crystal-phase XRD patterns were collected on a Philips PW3830 X-ray diffractometer using Cu-kα radiation ($\lambda$ = 0.15406 nm). The current was 40 mA and the voltage was 40 kV. The intensity data were collected at 25°C in the 2θ range from 5°to 90°with a scan rate of $1.20^o\ min^{-1}$.

TEM analyses were performed on a high-resolution Hitachi JEM-2100F operating at 200 kV to obtain information of the average particle size and the size distribution of the catalysts prepared.

XPS analysis was conducted using a Kratos AXIS Ultra $^{DLD}$ electron spectrometer to determine the surface composition with Al K X-ray anode source (hν=1486.6 eV) at 250 W and 14.0 kV.

### *2.3 Electrochemical measurements*

Electrochemical measurements were conducted through CV and LSV techniques using a potentiostat CHI 760 electrochemical analyzer. A conventional three-compartment electrochemical cell was employed for all electrochemical tests, in which a saturated calomel electrode (SCE) was used as the reference electrode and a platinum foil was used as the counter electrode. A rotating disk electrode (RDE) made of glassy carbon (GC) electrode with a diameter of 6.0 mm (corresponding to a geometric surface area of 0.283 $cm^2$, Pine, 5908Triangle Drive, Raleigh, NC)

was used as the working electrode, on which a layer of the studied catalysts was casted. The working electrode was coated with catalysts using the following steps: 4 mg of the NiPc/C catalyst was suspended in 2 mL of methanol/Nafion® solution (50:1 in mass) to form a catalyst ink, which was ultrasonically dispersed for 10 min. Then, 10 µL of the suspension was pipetted onto the surface of the GC electrode and then dried at room temperature for testing. The catalyst loading of each electrode was 70.6 µg $cm^{-2}$. All measured potentials were converted into the values referring to a standard hydrogen electrode (SHE).

RDE measurements were performed in 0.1 M KOH solution at room temperature. For every test, CV was first carried out by scanning the disk potential from -0.3 to 0.6 V at a scan rate of 50 mV $s^{-1}$ to examine the surface behavior of the catalyst in $N_2$-saturated 0.1 M KOH solution. Then $O_2$ was bubbled into the solution to form an $O_2$-saturated solution for ORR measurement. For more quantitative measurements of ORR activity of the catalysts, LSV was performed in the potential range between -0.7 and 0.2 V in $O_2$-saturated 0.1 M KOH solution at desired rotating rates. In order to ensure a steady state at each point of the LSV curves, a slow sweeping rate of 5 mV $s^{-1}$ was applied.

## 3. Results and discussion

*3.1 Electrochemical activity of NiPc/C catalysts towards ORR*

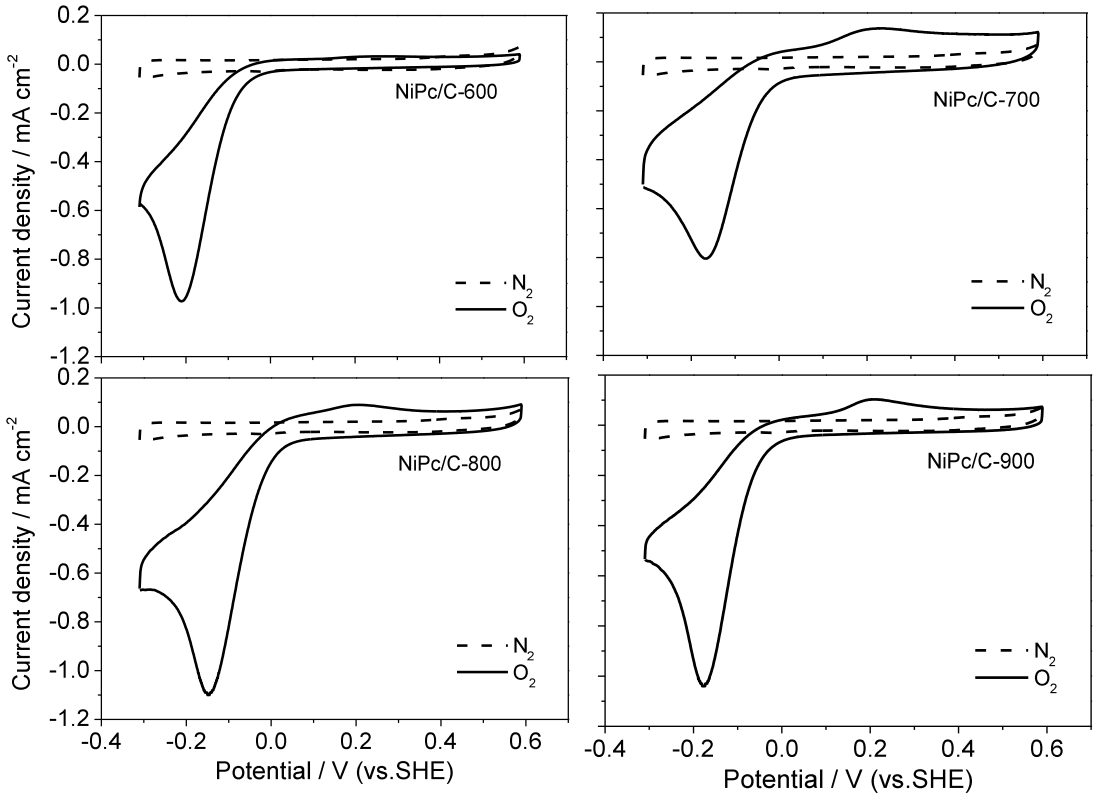

Figure 1. Cyclic voltammograms of the NiPc/C catalysts heat-treated at different temperatures in $N_2$-saturated and $O_2$-saturated 0.1 M KOH at room temperature. Scan rate: 50 mV $s^{-1}$,

Although the catalyzed ORR mechanisms of MPc catalysts are still not fully understood, there has been a general agreement in the literature that heat-treatment can effectively improve the electrocatalytic activity of the catalysts. In order to pursue the best catalytic performance for ORR, the influence of heat-treatment on the catalytic activity of NiPc/C catalysts was investigated by CV and LSV. Figure 1 shows the CV curves of $N_2$-saturated and $O_2$-saturated 0.1 M KOH solution obtained with the GC electrode coated with NiPc/C catalysts. It can be seen that there is no reduction peaks of oxygen at the NiPc/C catalyst electrodes in $N_2$-saturated 0.1 M KOH solution. However, clear reduction peaks are observed in $O_2$-saturated 0.1 M KOH solution for all NiPc/C catalysts after heat-treatment at various temperatures: -0.21 V for NiPc/C-600, -0.17 V for NiPc/C-700, -0.15 V for NiPc/C-800 and -0.17 V for NiPc/C-900, respectively. In addition, the ORR peak current density changes with increasing the heat-treatment temperature and reaches a maximum value at 800°C. Among all the curves in Figure 1, there is no peak attributed to the Ni $^{3+}/^{2+}$ redox, which indicates that the element nickel is in some other state, rather than nickel ions adsorbed on the carbon surface.

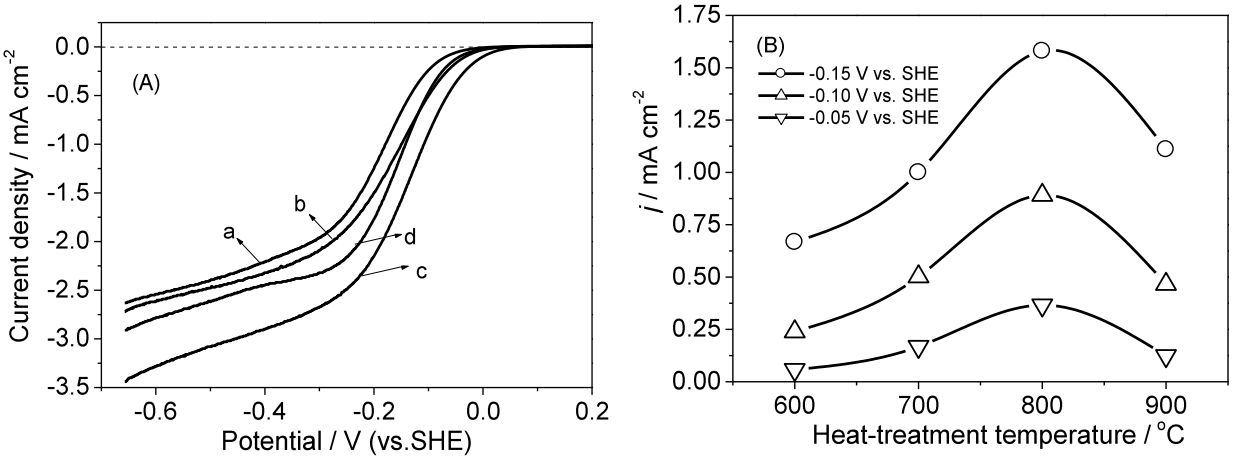


Figure 2. (A) Current-voltage curves for ORR catalyzed by NiPc/C catalysts heat-treated at (a) 600°C, (b) 700°C, (c) 800°C and (d) 900°C measured in $O_2$-saturated 0.1 M KOH at the scan rate 5 mV $s^{-1}$. Electrode rotating rate: 1500 rpm. (B) Current densities at -0.05, -0.10 and -0.15 V vs. SHE as a function of catalyst heat-treatment temperature with data obtained from (A).

In order to investigate the eletrocatalytic activity of NiPc/C catalysts for the ORR after heat-treatment at different temperatures, LSV was carried out using RDE coated with NiPc/C catalysts heat-treated at 600, 700, 800 and 900°C, respectively, and the polarization curves obtained are shown in Figure 2(A). It can be seen that for catalyst samples heat-treated at 600, 700 and 900°C, the onset potentials for the ORR are all located near 0.03 V, which are lower than that of the sample heat-treated at 800°C (near 0.05 V). The same trend can also be observed in the half-wave potentials

of the catalysts, which are: NiPc/C-800 (-0.15 V) > NiPc/C-700 ≈ NiPc/C-900 (-0.17 V) > NiPc/C-600 (-0.21 V), suggesting that ~800°C may be the optimal temperature in obtaining the most active electrocatalyst for ORR.

To further verify the heat-treatment temperature effect on the ORR activity, the current densities at -0.15, -0.10 and -0.05 V are plotted as the function of temperatures and, the results are shown in Figure 2(B). As can be seen, the current density increases significantly with increasing the heat-treatment temperature from 600°C to 800°C. Above 800°C, the current density decreases again and shows the lowest value when the heat-treatment temperature for the catalyst synthesis is at 900°C. The phenomenon clearly indicates that below 800°C, more ORR active sites in the NiPc/C catalyst could be produced. While, when temperature is high enough such as at 900°C, a portion of the active sites may be damaged to form other structures such as metallic nickel or nickel carbide, which are less active for ORR. These will be discussed throughly below. According to the curves shown in Figure 2(B), we can conclude that the optimal heat-treatment temperature is around 800°C. Therefore, in the subsequent study the NiPc/C obtained at 800°C was selected as the target catalyst.

*3.2 Kinetic study of the ORR catalyzed by heat-treatment NiPc/C*

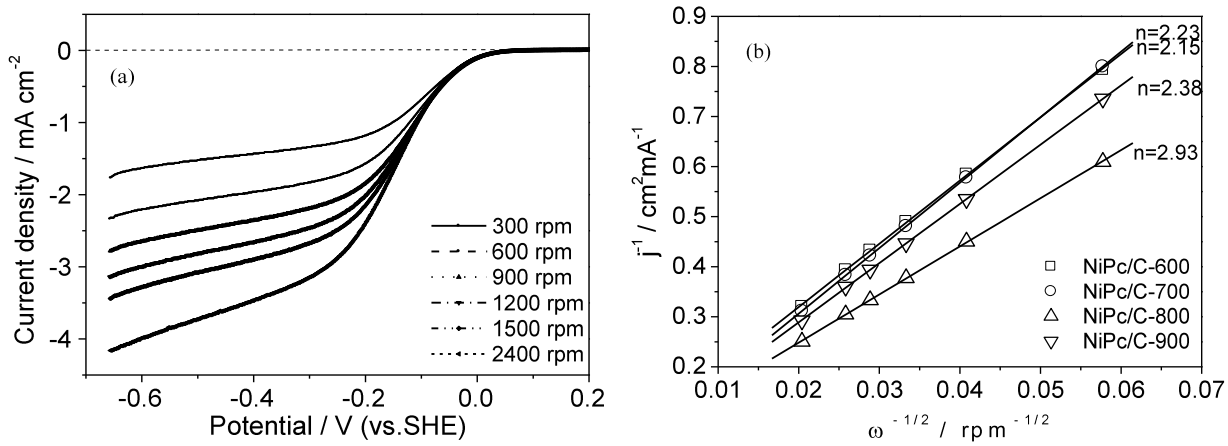


Figure 3 (a) Current-voltage curves at various electrode rotating rates obtained with NiPc/C-800 catalyst in $O_2$-saturated 0.1 M KOH at the scan rate 5 mV $s^{-1}$. (b) Koutecky-Levich plots for the ORR at –0.6 V vs. SHE from the current-voltage curves recorded at the same conditions as those in Figure 3(a) using catalysts obtained at various heat-treatment temperatures.

In order to further explore the kinetics of ORR catalyzed by NiPc/C in alkaline media, LSV data obtained at various rotation rates were processed using the Koutecky-Levich (K-L) equations[23]:

$$i_k = i \cdot i_d/(i_d - i) \text{ ----------(1)}$$

$$i_d = B\omega^{1/2} \text{----------(2)}$$

$$B = 0.2nFSCo_2Do_2^{2/3}v^{-1/6} \text{ --------(3)}$$

Where $B$ is the Levich slope, $\omega$ is the rotation rate, $n$ is the electron transfer number per oxygen molecule, $F$ is Faraday constant, S the electrode geometric surface area, $C_O$ is the concentration of oxygen, $D_O$ is the diffusion coefficient of $O_2$ in the electrolyte, $v$ is the kinetic viscosity and the constant 0.2 is adopted when rotation speed is expressed in revolutions per minute. Figure 3(a) shows the polarization curves at various rotation rates for ORR on the GC electrode coated with NiPc/C-800 in $O_2$-saturated 0.1 M KOH solution as a typical candidate. It can be seen that the limiting current for ORR increases with the rotation rate, while the onset potential of the catalyst for ORR remains unchanged. Figure 3(b) shows Koutecky-Leivich plots at -0.6 V, which indicates the estimation of overall electron number (n) transferred per oxygen molecule. For a better comparison, Koutecky-Leivich plots of NiPc/C catalysts heat-treated at other temperatures are also depicted in Figure 3(b). From the slopes of the Koutecky-Leivich plots, the electron transfer numbers per oxygen molecule in the overall reduction process can be calculated, and it was found that it changes with increasing the heat-treatment temperature: 2.23 for NiPc/C-600, 2.15 for NiPc/C-700, 2.93 for NiPc/C-800 and 2.38 for NiPc/C-900. These data suggest that the ORR catalyzed on NiPc/C-600, NiPc/C-700 and NiPc/C-900 electrodes is mainly a $2e^-$ reduction process leading to a large amount of $H_2O_2$. However, For NiPc/C-800 electrode, the electron transfer number is 2.93, which lies between the $2e^-$ and $4e^-$ reduction process, suggesting a great affect on the decreasing of $H_2O_2$ by heat-treatment at 800°C.

*3.3 Studies on the acitve site structures of the NiPc/C catalysts*

Figure 4 shows the TG and DTG curves for $H_2Pc/C$ and NiPc/C, respectively. As shown in Figure 4(a), $H_2Pc/C$ shows only one major peak at 550°C with a weight loss of about 30 wt%, indicative of the decompsition of $H_2Pc$ [19]. In the case of NiPc/C, situations are different. The DTG curve of NiPc/C shows three peaks at around 150, 560 and 760°C (Figure 4(b)). Corresponding to DTG, there are three steps on the curve of TG: (1) the first step starts at 130°C to reach a plateau near 250°C with a weight loss of about 7.5 wt%. In this stage, NiPc has a stable molecular structure and a small amount of weight is lost due to volatilization of absolute ethanol and water molecules. (2) the second step starts at 500°C and ends at 610°C with 10.5 wt% weight loss which may corresponds to the release of NiPc/C on the carbon surface. (3) the decomposition of NiPc/C chelate happens at a temperature above 610°C. The catalytic activities of NiPc/C-700, NiPc/C-800 and NiPc/C-900 are all much higher than that of NiPc/C-600, which indicates that catalytic active sites are probably formed at the third step. Furthermore, the total mass loss of NiPc/C is smaller than that of $H_2Pc/C$ by about 12%. This implies that Ni species prevents phthalocyanine from thermal decomposition and leads to higher nitrogen content which are helpful to form more ORR activity sites.

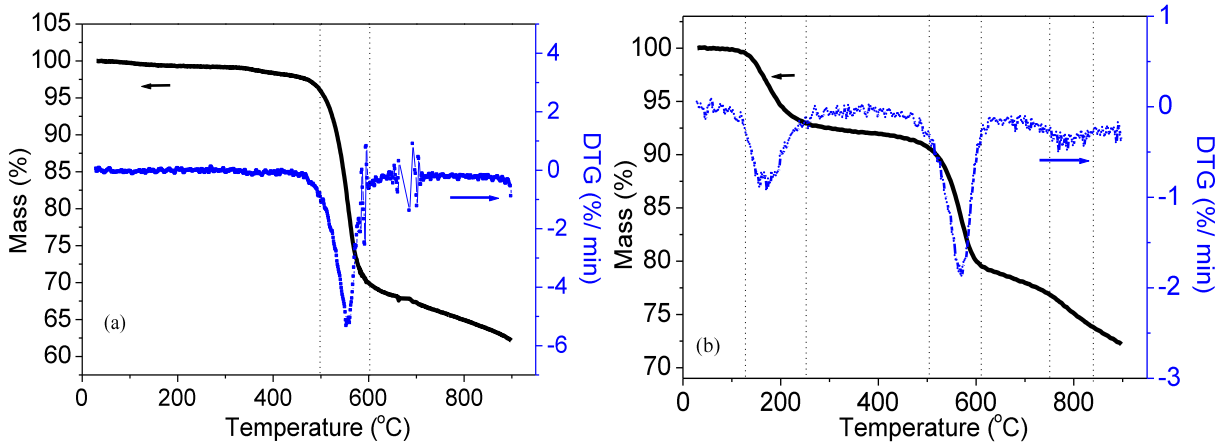


Figure 4. TG/DTG curves of (a) $H_2Pc/C$ and (b) NiPc/C, respectively

XRD analyses were conducted to obtain crystallographic information on the NiPc/C catalysts. Figure 5 shows the XRD patterns of NiPc/C catalysts after heat-treatment at 600, 700, 800 and 900°C, respectively. The first large broad peak located at about $2\theta = 25^{o}$ in all the XRD patterns can be assigned to the strong graphite character of the Vulcan XC-72. It can also be clearly seen that NiPc/C-600 shows only one and broad peak at 44.5°, which is assigned to the Ni (111) peak. However, when heat-treatment temperature is increased from 700 to 900°C, two new diffraction peaks at 51.8° and 76.3°, respectively, appeared, indicating the occurrence of the decomposition of NiPc/C structure during the heat-treatment process and the aggregating of the metallic nickel. These two peaks centered at 51.8° and 76.3° are corresponding to the Ni (200) peak and Ni (220) peak, and these two peaks become sharpened with the increase in heat-treatment temperature, which suggests that Ni clusters grow at higher pyrolyzing temperature.

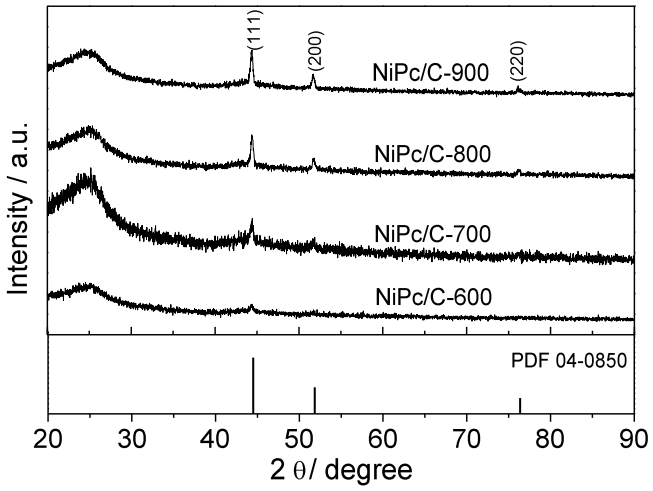


Figure 5. XRD patterns of NiPc/C catalysts heat-treated at 600, 700, 800 and 900°C, respectively.

Another confirmation of the presence of metallic Ni in the NiPc/C catalysts heat-treated at different temperatures can be seen from Figure 6, in which TEM images of the NiPc/C obtained at 600, 700, 800 and 900°C heat-treatment are illustrated. As seen in Figure 6a, no clear metal particles appear for the catalyst heat-treated at 600°C except for some aggregates with an average particle size of 50 nm on the carbon support surface. When the catalyst is heat-treated at 700°C, the aggregate size decreases, and a smaller size of the particle cluster is observed with an average size of about 30 nm (Figure 6b). It is worth to mention that the TEM images of the NiPc/C catalyst samples heat-treated at 600 and 700°C give no conspicuous indication of metallic Ni aggregation, however, the TEM image of the samples heat-treated at 800 and 900°C clearly show the metallic Ni aggregation (Figure 6c and 6d). For example, some black dots with an average size of about 25 nm can be observed in the NiPc/C sample heat-treated at 800°C, and the NiPc/C after heat-treatment at 900°C shows a heavily agglomerated material of nano-sized particles (with an average particle size of 60 nm). The NiPc/C is in a highly crystalline phase (the Ni crystallites growth) after high-temperature treatment. These results suggest that heat-treatment can decompose the NiPc/C to metallic Ni, which then agglomerates into large particles when the heat-treatment temperature is increased. This result is in agreement with the observation from the XRD analysis in Figure 5. Generally, metallic Ni is not active for the ORR. Hence, to prevent the formation of metallic Ni in the catalyst, the heat-treatment should be conducted not at a too high temperature. As shown in Figure 2, NiPc/C catalyst sample heat-treated at 800°C shows the best ORR activity, indicating that a lot of active sites may be formed at this temperature, although some small metallic Ni particles are observed. In order to gain some information on active sites of the catalysts as-prepared, the surface characterization of NiPc/C catalysts after heat-treatment at 800°C was carried out by XPS.

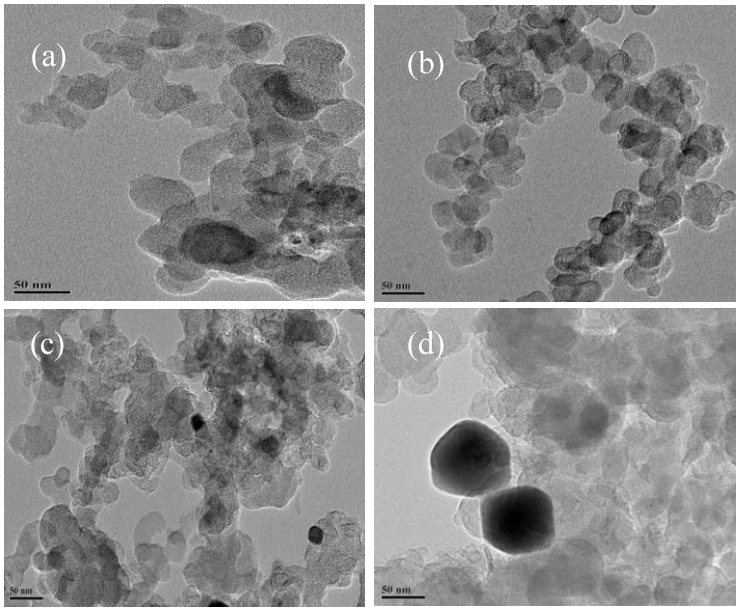


Figure 6. TEM images for NiPc/C catalyst heat-treated at (a) 600°C, (b) 700°C, (c) 800°C and (d) 900°C, respectively.

Figure 7 shows the N 1s spectral region for NiPc/C-800, where the N signal is divided into four bands, marked $N_I$, $N_{II}$, $N_{III}$, and $N_{IV}$, respectively. The $N_I$ band at lower binding energy of 398.8 eV could be assigned to pyridinic-N, the $N_{II}$ band at 399.9 eV and the $N_{III}$ band at 401.2 eV may be related to pyrrolic-N and graphitc-N, respectively. Finally, the broader $N_{IV}$ band at 404.3 eV could be attributed to N-O bonds (pyridine-N-oxide) [24-26]. According to literatures, pyridine-N and graphitic-N are believed to play important roles in determining the electrocatalytic ORR activity and stability of macrocycles, while pyridine-N-oxide seems useless in improving the activity [27,28]. In the case of NiPc/C-800, it can be clearly seen that both pyridinic-N and graphitic-N are the major bands in this sample forming the ORR active sites, although pyridine-N-oxide can be observed also. Sidik *et al.* [29] once observed that graphitic-N could catalyze the ORR through a $4e^-$ pathway. That is why we observed the high ORR activity catalyzed by NiPc/C-800 catalyst. This study may at least partially explain the results that the electron transfer number of NiPc/C-800 is higher than NiPc/C catalysts heat-treated at other temperatures. Therefore, it can be concluded that both pyridinic-N and graphitic-N bonded by Ni ions should be mainly responsible for the enhanced ORR activity in this work.

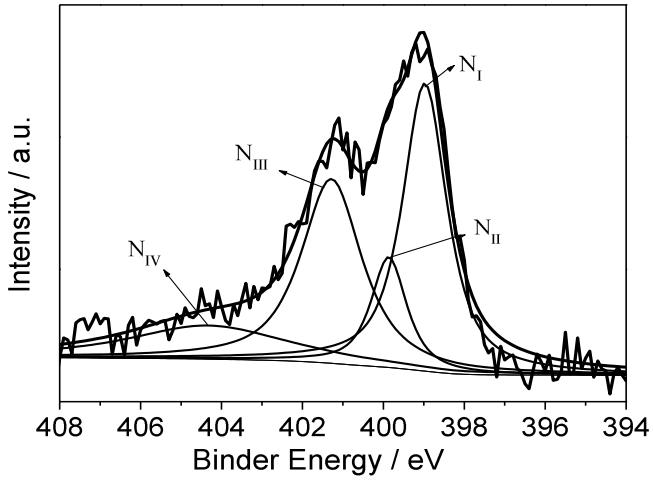


Figure 7. XPS spectra in the N 1s region for the NiPc/C catalysts heat-treated at 800°C.

**4. Conclusions**

In conclusion, carbon-supported NiPc/C catalyst as an novel cahode catalyst for ORR has been succefussly prepared by solvent-impregnation along with the high-temperature treatment. A significant influence of the heat-treatment was found on the catalytic activity of the NiPc/C catalysts for ORR. The catalyst heat-treated at 800 °C displayed significantly improved activity through RDE and CV measurements in oxygen-saturated alkaline electrolyte at room temperature. The number of electrons transferred during the ORR varies with increasing the heat-treatment

temperature: 2.23 at 600°C, 2.15 at 700°C, 2.93 at 800°C and 2.38 at 900°C. XRD and TEM clearly confirm that the depositions of nanometallic Ni with different sizes are produced with heat-treatment temperature, which are not active for ORR. XPS analysis reveals that both pyridinic-N and graphitic-N should be the active sites responsible for the enhanced ORR activity. Here, the catalytic activity of NiPc/C is still low in comparison with reported Co- and Fe-centered phthalocyanines [17]. However, these initial results are promising for the application in alkaline fuel cells. It is believed that by further optimizaiton of the experimental conditions, such as using other synthetic method, modification with metal or nitrogen precursers, both the catalytic activity and the selectivity of NiPc/C could be improved further.

## 5. Akcnowledgements

We give our thanks to the financial support from the National Natural Science Foundation of China (21173039), Specialized Research Fund for the Doctoral Program of Higher Education, SRFD (20110075110001), the Opening Foundation of Zhejing Provincial Top Key Discipline and the Shanghai Leading Academic Discipline Project (B604) Fund.

## 6. References

[1] S. Sharma, A. Ganguly, P. Papalonstantinou, X. Miao, M. Li, J. L. Hutchison, M. Delichatsios and S. Ukleja, J. Phys. Chem. C, 114, 19459 (2010).

[2] B. Wang, J. Power Source, 152, 1 (2005).

[3] N. Wagner, M. Schulze and E. Gülzow, J. Power Source, 127, 264 (2004).

[4] C. Coutanceau, L. Demarconnay and J.−M. Léger, J. Power Source, 156, 14 (2006).

[5] M. Zhiani, H. A. Gasteiger, M. Piana and S. Catanorchi. Int. J. Hydrog. Energy, 36, 5110 (2011).

[6] H. Schulenburg, S. Stankov, V. Schünemann, J. Radnik, I. Dorbant, S. Fiechter, P. Bogdanoff and H. Tributsch, J. Phys. Chem. B, 107, 9034 (2003).

[7] L. Jiang, A. Hsu, D. Chu and R. Chen, J. Electrochem. Soc., 156, B370 (2009).

[8] S. Lj. Gojković, S. Gupta and R. F. Savinell, J. Electroanal. Chem., 462, 63 (1999).

[9] C. Song, L. Zhang and J. Zhang, J. Electroanal. Chem., 587, 293 (2006).

[10] M. Lefèvre and J. P. Dodelet, Electrochim. Acta, 48, 2749 (2003).

[11] R. Baker, D. P. Wilkinson and J. Zhang. Electrochim. Acta, 53, 6906 (2008).

[12] G. Lalande, G. Tamizhmani, R. Côté, L. Dignard-Bailey, M. L. Trudeau, R. Schulz, D. Guay and J. P. Dodelet, J. Electrochem. Soc., 142, 1162 (1995).

[13] G. Faubert, G. Lalande, R. Côté, D. Guay, J. P. Dodelet, L.T. Weng, P. Bertrand and G. Dénès, Electrochim. Acta, 41, 1689 (1996).

[14] M. Lefèvre, E. Proietti, F. Jaouen and J. P. Dodelet, Science, 324, 71 (2009).

[15] Y. Lu and R. G. Reddy. Electrochim. Acta, 52, 2562 (2007).

[16] I. Kruusenberg, L. Matisen, Q. Shah, A. M. Kannan and K. Tammeverski, Int. J. Hydrogen. Energy, 37, 4406 (2012).

[17] R. Chen, H. Li, D. Chu and G. Wang, J. Phys. Chem. C, 113, 20689 (2009).

[18] V. Bambagioni, C. Bianchini, J. Filippi, A. Lavacchi, W. Oberhauser, A. Marchionni, S. Moneti, F. Vizza, R. Psaro, V. Dal Santo, A. Gallo, S. Recchia and L. Sordelli, J. Power Source, 196, 2519 (2011).

[19] Y. Nabae, S. Moriya, K. Matsubayashi, S. M. Lyth, M. Malon, L. Wu, N. M. Islam, Y. Koshigoe, S. Kuroki, M. Kakimoto, S. Miyata and J. Ozaki, Carbon, 48, 2613 (2010).

[20] C. W. B. Bezerra, L. Zhang, K. Lee, H. Liu, A. L. B. Marques, E. P. Marques, H. Wang and J. Zhang, Electrochim. Acta, 53, 4937 (2008).

[21] J. Ozaki, S. Tanifuji, N. Kimura, A. Furuichi and A. Oya, Carbon, 44, 1298 (2006).

[22] N. Sehlotho and T. Nyokong, J. Electroanal. Chem., 595, 161 (2006).

[23] A. J. Bard and L. R. Faulkner, Electrochemical Methods, Fundamentals and Applications, 2nd ed., John Wiley & Sons, Inc., N. Y., (2000).

[24] P. Wang, Z. Ma, Z. Zhao and L. Jia, J. Electroanal. Chem., 611, 87 (2007).

[25] A. Velázquez-Palenzuela A, L. Zhang, L. Wang, P. L. Cabot, E. Brillas, K. Tsay and J. Zhang, J. Phys. Chem. C, 115, 12929 (2011).

[26] G. Liu, X. Li, P. Ganesan and N. B. Popov, Electrochim. Acta, 55, 2853 (2010).

[27] X. Li, G. Liu and N. B. Popov, J. Power Source, 195, 6373 (2010).

[28] K. Lee, L. Zhang, H. Liu, R. Hui, Z. Shi and J. Zhang, Electrochim. Acta, 54, 4704 (2009).

[29] A. R. Sidik, B. A. Anderson, P. N. Subramanian, P. S. Kumaraguru and N. B. Popov, J. Phys. Chem. C, 110, 1787 (2006).